PHYSICAL REVIEW B **96**, 041301(R) (2017)

Electrical and optical switching in the bistable regime of an electrically injected polariton laser

M. Klaas,[1] H. Sigurdsson,[2] T. C. H. Liew,[3] S. Klembt,[1] M. Amthor,[1] F. Hartmann,[1] L. Worschech,[1] C. Schneider,[1] and S. Höfling[1,4]

[1]*Technische Physik, Wilhelm-Conrad-Röntgen-Research Center for Complex Material Systems, Universität Würzburg, Am Hubland, D-97074 Würzburg, Germany*

[2]*Science Institute, University of Iceland, Dunhagi-3, IS-107 Reykjavik, Iceland*

[3]*Division of Physics and Applied Physics, Nanyang Technological University, 637371, Singapore*

[4]*SUPA, School of Physics and Astronomy, University of St Andrews, St Andrews KY16 9SS, United Kingdom*

(Received 14 February 2017; published 10 July 2017)

We report on electrically and nonresonant optically induced switching in the bistable regime of an electrically pumped polariton laser. Electrical switching effects can be observed by adding controlled noise in the electrical pump of the system. Noise is expected to influence the hysteresis characteristics of a bistable device and determines its application robustness. We find that the hysteresis width decreases symmetrically with a linear dependency until we observe a quenching of the bistability at a certain noise level and the output of the system becomes monostable. Furthermore, we explore the possibility to switch between the two bistable branches by a nonresonant optical pulse. Our experimental findings can be described by a set of rate equations modeling the population dynamics with additional noise terms.

DOI: 10.1103/PhysRevB.96.041301

Introduction. Exciton-polaritons are light-matter quasiparticles created in a microcavity system in the strong coupling regime [1,2]. Since polaritons are bosons in the presence of gain and loss, they can form a dynamic quasicondensate in a distinct energy state [3,4]. The emission from such a condensate shows properties resembling a conventional laser [5] including good temporal [6,7] and spatial [3,8,9] coherence. As polariton lasing does not necessarily rely on population inversion, thresholds up to two magnitudes below conventional vertical-cavity surface-emitting laser (VCSEL) devices are possible [10]. Adding the fact that condensation can be observed at room temperature in semiconductors such as GaN [11], ZnO [12], and organic materials [13–15], makes the polariton laser an attractive next-generation device. For many future applications, an electrical injection scheme is a necessary prerequisite [16,17].

Polariton condensates are also of fundamental interest due to their interesting relaxation and formation mechanism. In a nonresonant pumping configuration, relaxation occurs from a long-lived reservoir towards the lower polariton branch [18]; at sufficient densities stimulated scattering [19] allows for the formation of this new coherent state. Furthermore, polariton condensates exhibit striking phenomena such as single- and half-quantum vortices [22,23], superfluidity [20], and quantum turbulence [21]. Since polaritons interact with their environment via their excitonic part [24], they enable energy-efficient switching processes in a variety of polariton waveguide based logical architecture elements [25–29], which promise highly integrated logic devices.

Optical bistability effects in semiconductors have also been proposed and used for applications in optical signal amplification [30,31] and can also potentially be used in all optical transistors and memories in an integrated optical circuit, demonstrated on a Si basis [32]. The advantages of such bistability-based devices are their simplicity, robustness, low-power operation [33], and high operation switching speed [34].

A variety of experimental bistable and multistable effects based on polaritons have already been reported [37–43]. Recently, subfemtojoule levels switching have been reached with a nonresonant electrical spin switch [35] and switching based on bistable polariton systems has been theoretically investigated [36]. Indeed, a nonresonant bistability in an electrically injected system [44] represents a much more application friendly driving scheme. In such a scheme, the switching times would be limited by the reservoir lifetimes, which typically range on the order of a few hundred picoseconds in GaAs [45].

The application of noise to a bistable system can induce transitions between the two states, and can lead to a variety of interesting effects. References [46,47] studied the possibility for stochastic resonance in a polariton system, in which a noisy excitation is used to coherently amplify the system response. The effects of noise on the bistability of an optically excited polariton condensate has been investigated in Ref. [48], in which a narrowing of the hysteresis has been observed for increased excitation noise.

In our experiment, we investigate the effect of controlled noise in addition to a direct electrical injection of polaritons and study its impact on the bistability properties of our device. We observe a direct correlation between the input noise and the bistable properties of our condensate, including the transition to complete monostable behavior upon a specific input noise. Furthermore, we demonstrate that it is possible to use a short nonresonant optical excitation pulse superimposed with the electrical injection to switch from the lower to the upper state of the two bistability branches.

Experiment. The investigated sample has 23 (27) doped AlAs/GaAs distributed Bragg reflectors (DBRs) above (below) its cavity [see Fig. 1(a)] and is comparable to the device that has been investigated in Ref. [16]. The top mirror is carbon doped, supporting the injection of holes and the bottom mirror is silicon doped for injection of electrons. The cavity is a λ thick, intrinsic GaAs spacer, which contains four InGaAs quantum wells (QWs) with a thickness of 8 nm. The QWs are arranged in a single stack in the vertical center of the cavity spacer. In order to facilitate efficient current injection and to provide an in-plane photonic confinement,

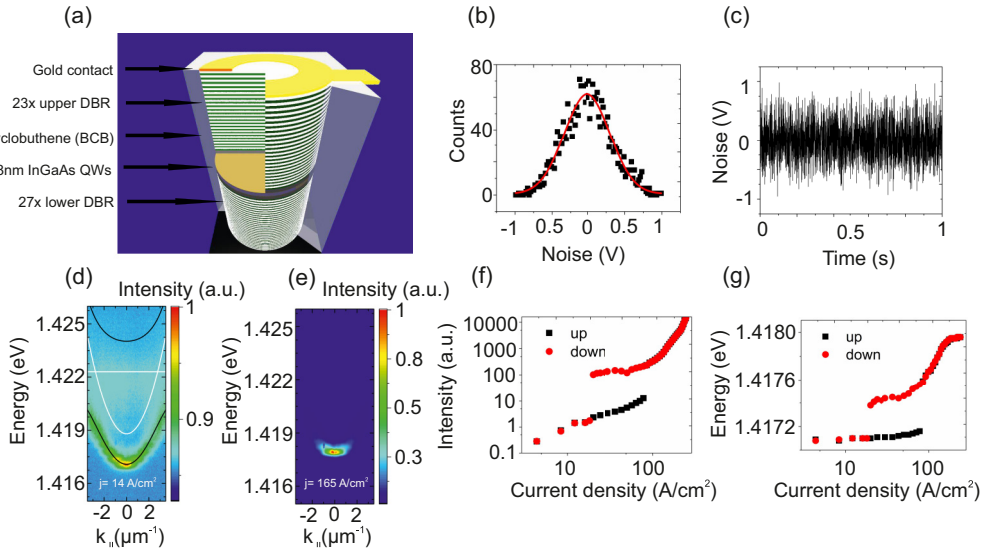

FIG. 1. (a) Sketch of the investigated device. (b), (c) Noise characteristics used in conjunction with a dc voltage. (d) Polariton dispersion below threshold at an injection current of $j = 14\,\mathrm{A/cm^2}$. The white lines show the exciton and photon modes, the black lines show the dispersions from a coupled oscillator model. (e) Polariton dispersion above threshold at an injection current of $j = 165\,\mathrm{A/cm^2}$. (f) Input-output intensity characteristics for sweeping the injection current up and down. (g) Peak energy of the ground-state emission from a Lorentz fit at $k = 0 \pm 0.1\,\mu\mathrm{m}^{-1}$ for both up and down current ramping respectively.

micropillars with a diameter of 20 μm were etched into the planar cavity. Subsequently, the sample has been planarized by a polymer [benzocyclobuthene (BCB)]. To implement the current injection, ring-shaped gold contacts were deposited onto the micropillar. A 10 μm diameter aperture has been left open to allow for decay of the polaritons out of the structure for investigation.

The device was put in a magnetocryostat, which was set to a magnetic field of 5 T. This magnetic field increases light-matter coupling [49] and has been shown to promote polariton relaxation [16]. The sample exhibits a Rabi splitting of 5.5 meV, which increases to approximately 6 meV at a magnetic field of 5 T. All experiments have been performed on the same micropillar device with a detuning of -3.5 meV, which corresponds to an exciton fraction of 25% and a photon fraction of 75% at 5 T. The Q factor was experimentally estimated for a micropillar device with high photonic content to be 6000 [16]. The measurements were performed at a temperature of 5 K.

The electrical noise in the experiment was provided by an arbitrary waveform generator Model 3390 from Keithley in a bias tee configuration with a standard dc voltage generator. The noise output characteristics are shown in Figs. 1(b) and 1(c). Figure 1(b) depicts a Gaussian noise distribution and Fig. 1(c), the time-resolved noise signal. The cut-off frequency of the arbitrary waveform generator is 20 MHz, which is on the order of the carrier lifetime. This timescale, however, is much longer than the polariton formation from the reservoir and decay, which takes place in picoseconds.

The noise strength is defined as the standard deviation of our Gaussian noise signal σ compared to the device hysteresis width ΔA. The optical measurements have been performed with an angle resolved Fourier space setup with the possibility for real space imaging [50].

Figure 1(d) shows the angle-resolved electroluminescence characteristics of our device. At a low injection current of $j = 14\,\mathrm{A/cm^2}$, the device operates in the linear regime. The luminescence follows the lower polariton branch, which is calculated with a standard coupled oscillator approach and plotted in Fig. 1(d) (black lines). At a current density of 78 $\mathrm{A/cm^2}$, stimulated scattering processes enable the formation of a polariton condensate. The emission from this condensate at an injection current of 165 $\mathrm{A/cm^2}$, centered around $k_\perp = 0\,\mu\mathrm{m}^{-1}$, is shown in Fig. 1(e). Figure 1(f) presents an input-output intensity characteristic of our device. It has been extracted from a Lorentzian fit of the integrated emission around $k_\perp = 0 \pm 0.1\,\mu\mathrm{m}^{-1}$. The emission properties show a jump at the first threshold in the intensity output and energy position. This is a commonly observed phenomenon in bistable systems. Moreover, Fig. 1(g) demonstrates a persistent blue shift after the first threshold. This evidences continued strong coupling conditions of the system, attributed to increased exciton-exciton interaction [51]. A second threshold at approximately 180 $\mathrm{A/cm^2}$ reveals itself in a second nonlinear intensity increase and a pinning of the emission energy, demarking photon lasing.

Figures 1(f), 1(g) show the hysteresis curve without any applied noise. The hysteresis width ΔA amounts in this case to 70 $\mathrm{A/cm^2}$. It is important to notice that this hysteresis width does not correspond to the true width without any external influences, since in every system there is an internal noise level.

The hysteresis itself shows a width reduction with increasing magnetic field and is absent under nonresonant optical pumping. Furthermore, the photon lasing threshold does not show a bistable character. The origin of the bistability has been previously explained by a dependence of the electron-hole tunneling lifetime on the carrier density, which creates a positive feedback loop [44].

Experiment. Since it is not self-evident that the system remains in the strong coupling regime with a high amount

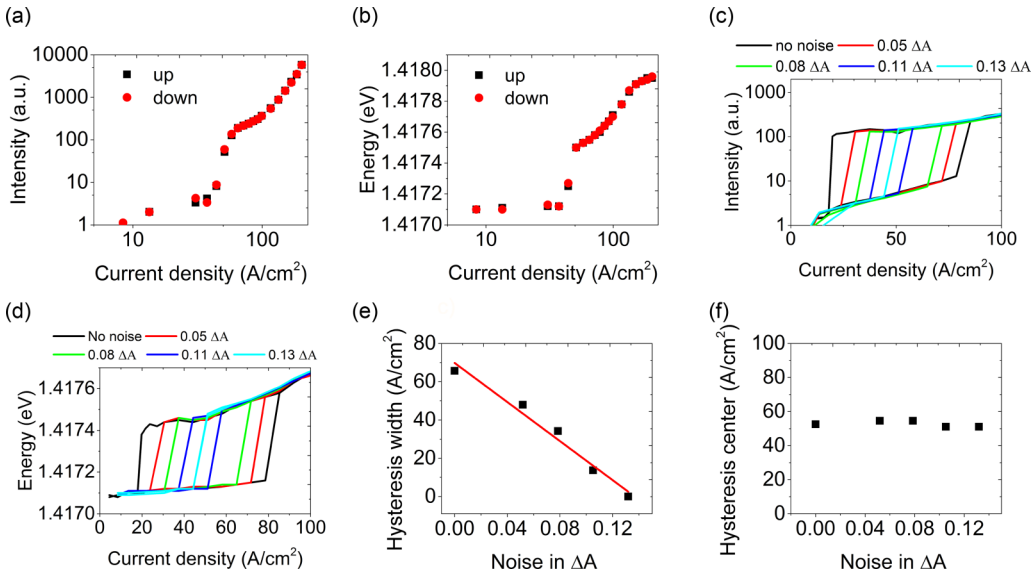

FIG. 2. (a), (b) Intensity/energy as a function of excitation current density with an applied noise strength of 0.21 ΔA. (c), (d) Input-output graphs of the polariton emission intensity/energy hysteresis cycle for 0–0.13 ΔA noise strengths. The hysteresis decreases until a threshold noise makes the system exhibit monostable behavior. (e) Hysteresis width as a function of injected noise. The dependence of hysteresis width on excitation noise is linear as shown with the red line fit. (f) Hysteresis center as a function of applied noise. Since the center does not shift with applied noise, the hysteresis decreases symmetrically.

of applied noise, Figs. 2(a) and 2(b) show the input-output characterization with a relatively high noise level of 0.21 ΔA. The analysis shows all the same features (continued blue shift, two-threshold behavior) as observed before, which supports the existence of an electrical polariton lasing regime with a high level of noise in the excitation current. It is also noticeable that the hysteresis has not only vanished, but it is possible to observe a gradual onset of polariton lasing at the first threshold under these conditions.

To analyze the hysteresis dependency on applied noise, we record the input-output curves for up and down current injection for a variety of noise levels. The results can be seen in Fig. 2(c). The hysteresis width decreases with increased applied noise. Figure 2(d) shows the corresponding emission energy analysis. At a noise level of 0.13 ΔA, we no longer observe a hysteresis, which means there exists a threshold noise for which the system loses its bistable character. Figure 2(e) shows the linear decrease of the hysteresis width with applied noise strength. As can be seen in Fig. 2(f), the center position of the hysteresis cycle does not change with noise (maximum deviation of 2 A/cm^2), meaning the hysteresis undergoes a symmetric narrowing process.

We will now address the properties of our bistable device at a magnetic field of 5 T under an additional nonresonant spectrally narrow cw excitation with a laser. Figure 3(a) depicts the excitation configuration, which takes advantage of the

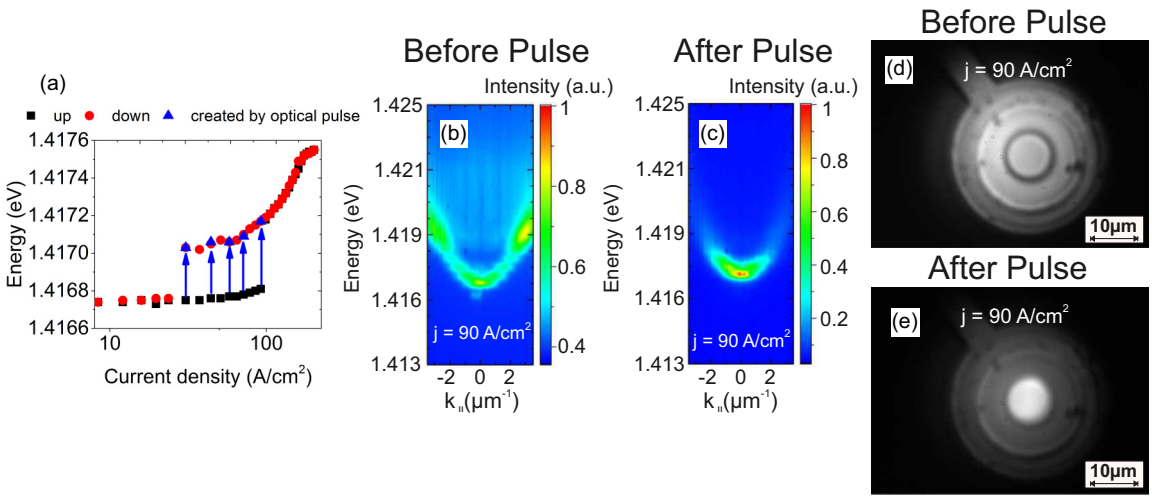

FIG. 3. (a) The graph shows the creation of artificial states in the upper bistability branch with a short external optical pulse in addition to a stable electrical injection current. (b), (d) and (c), (e) are the dispersion relations/real space images of the polariton emission before and after the nonresonant optical pulse with a constant applied current of $j = 90\,\mathrm{A/cm^2}$.

bistability in combination with an optical excitation to trigger the bistable state of the lower polariton branch (indicated by arrows). It is implemented by injecting additional free carriers with a nonresonant laser at a wavelength of 658 nm, which was applied for various seconds (0.5 mW peak power).

The laser is spectrally far off resonance with the emission wavelength of the polariton condensate at 874 nm and therefore introduces hot carriers into the system. The laser is positioned in the center of the ring contact, while an injection current in the bistable regime of the lower branch is applied. A pulse of the laser then triggers the polariton condensate emission on the upper bistable branch, which is indicated by the blue arrows in Fig. 3(a). This emission persists as the laser is switched off. These switched states have exactly the same emission properties as can also be observed by simple electrical injection at the upper bistability branch. Figures 3(b) and 3(c) present the dispersion relation before and after the nonresonant optical pulse, where Fig. 3(c) clearly shows a condensate emission characteristic. Figure 3(d) displays the real space image of the emitting micropillar device with a constant applied injection current illuminated by white light. In Fig. 3(e), the optical excitation pulse has switched on the electrical polariton condensate. The significant relative increase in emission intensity indicates the polariton condensate state.

In the case when the system is driven with a noisy excitation, this optical switching is only observable in the remaining area of the hysteresis. Once the hysteresis quenches, optical switching is no longer observed.

Theory. The bistability in our system has been previously described by a density-dependent renormalization of the decay rate of high energy carriers in Ref. [44]. In this approach, we describe the system as a set of rate equations that model the relaxation dynamics between the carrier reservoir, the exciton population, and the polaritons in the system. These population dynamics crucially depend on the carrier decay rate. This carrier decay rate in turn depends on the carrier population already present in the active region, due to their screening of the internal electric field. This loss rate dependency on the carrier population generates the positive feedback effect, which is responsible for the existence of a bistability in our polaritonic system. The details are given in the Supplemental Material [52], where the theoretical model was extended to include Gaussian noise in the electrical pumping via a distributed random variable in the excitation term.

Figure 4(a) shows the results of modeling, including the analytical stationary solution in the absence of noise (solid black curve) and numerically obtained hysteresis curves in the presence of noise. As in the experiment, we observe a significant narrowing of the hysteresis curve with increasing

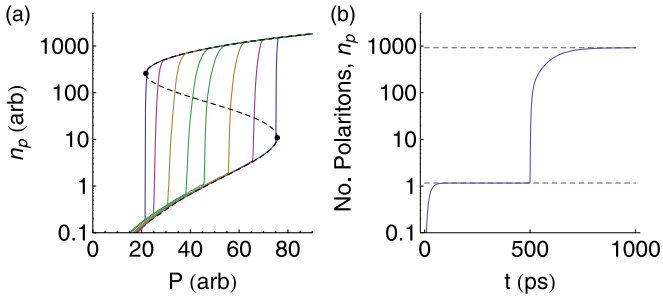

FIG. 4. (a) Theoretical dependence of the polariton density on the pumping rate, with different levels of noise added stochastically to the system. The solid black curve shows the stationary state, obtained in the absence of noise with turning points at the positions of the black spots. (b) Theoretical switching process with an optical pulse at $t = 500$ ps, triggering the polariton condensate.

noise. Furthermore, the model allows the simulation of the nonresonant optical switching process. Figure 4(b) shows theoretical simulation of the time-dynamics of the system for a pump power in the middle of the hysteresis zone. The system initially forms in a low-density state, but the addition of a nonresonant pulse at $t = 500$ ps causes switching to the high-power branch of the hysteresis curve.

Conclusion. We have demonstrated the possibility to fine tune the hysteresis width of an electrical polariton laser with a controlled noise input. Furthermore, the origin of the bistability in the carrier reservoir makes it possible to switch from the lower of the two bistable polariton emission states to the upper one by nonresonant optical injection of additional carriers to produce the necessary positive feedback effect. The theoretical description based on coupled rate equations with a simulated stochastic noise term explains the observed phenomena and matches the experiment. These results can be used as a first guiding point for the noise analysis of electrically driven polariton coherent light sources and especially for the robustness of a bistability based logic encoding. Additionally, they give fundamental insight into the nature of a nonresonant optical bistability due to an electrical polariton injection scheme and provide the possibility for further investigation of electrical polariton bistability devices to serve as a next-generation logic architecture.

Acknowledgments. The authors would like to thank the State of Bavaria for financial support. We thank M. Lermer and A. Wolf for support in sample fabrication. H.S. acknowledges support from The Icelandic Research Fund, Grant No. 163082-051. T.L. thanks the Ministry of Education (Singapore) Academic Research Fund for support. C.S. and M.K. thank the DFG within the project Schn1376-3.1.

[1] C. Weisbuch, M. Nishioka, A. Ishikawa, and Y. Arakawa, Phys. Rev. Lett. **69**, 3314 (1992).

[2] A. Kavokin, J. Baumberg, G. Malpuech, and F. Laussy, *Microcavities* (Clarendon, Oxford, 2006).

[3] J. Kasprzak, M. Richard, S. Kundermann, A. Baas, P. Jeambrun, J. M. J. Keeling, F. M. Marchetti, M. H. Szymanska, R. Andre, J. L. Staehli, V. Savona, P. B. Littlewood, B. Deveaud, and L. S. Dang, Nature (London) **443**, 409 (2006).

[4] R. Balili, V. Hartwell, D. Snoke, L. Pfeiffer, and K. West, Science **316**, 1007 (2007).

[5] A. Imamoglu, R. J. Ram, S. Pau, and Y. Yamamoto, Phys. Rev. A **53**, 4250 (1996).

[6] S. Kim, B. Zhang, Z. Wang, J. Fischer, S. Brodbeck, M. Kamp, C. Schneider, S. Höfling, and H. Deng, Phys. Rev. X **6**, 011026 (2016).
[7] M. Amthor, H. Flayac, I. G. Savenko, S. Brodbeck, M. Kamp, T. Ala-Nissila, C. Schneider, and S. Höfling, arXiv:1511.00878.
[8] H. Deng, G. S. Solomon, R. Hey, K. H. Ploog, and Y. Yamamoto, Phys. Rev. Lett. **99**, 126403 (2007).
[9] J. Fischer, I. G. Savenko, M. D. Fraser, S. Holzinger, S. Brodbeck, M. Kamp, I. A. Shelykh, C. Schneider, and S. Höfling, Phys. Rev. Lett. **113**, 203902 (2014).
[10] H. Deng, G. Weihs, D. Snoke, J. Bloch, and Y. Yamamoto, PNAS **100**, 15318 (2003).
[11] S. Christopoulos, G. Baldassarri Hger von Hgersthal, A. J. D. Grundy, P. G. Lagoudakis, A. V. Kavokin, J. J. Baumberg, G. Christmann, R. Butte, E. Feltin, J. Carlin, and N. Grandjean, Phys. Rev. Lett. **98**, 126405 (2007).
[12] T. Lu, Y. Lai, Y. Lan, S. Huang, J. Chen, Y. Wu, W. Hsieh, and H. Deng, Opt. Express **20**, 5530 (2012).
[13] J. D. Plumhof, T. Stoferle, L. Mai, U. Scherf, and R. F. Mahrt, Nat. Mater. **13**, 247 (2014).
[14] K. S. Daskalakis, S. A. Maier, R. Murray, and S. Kena-Cohen, Nat. Mater. **13**, 271 (2014).
[15] C. P. Dietrich, A. Steude, L. Tropf, M. Schubert, N. M. Kronenberg, K. Ostermann, S. Höfling, and M. C. Gather, Sci. Adv. **2**, 1600666 (2016).
[16] C. Schneider, A. Rahimi-Iman, N. Y. Kim, J. Fischer, I. G. Savenko, M. Amthor, M. Lermer, A. Wolf, L. Worschech, V. D. Kulakovskii, I. A. Shelykh, M. Kamp, S. Reitzenstein, A. Forchel, Y. Yamamoto, and S. Hoefling, Nature (London) **497**, 348 (2013).
[17] P. Bhattacharya, B. Xiao, A. Das, S. Bhowmick, and J. Heo, Phys. Rev. Lett. **110**, 206403 (2013).
[18] D. Porras, C. Ciuti, J. J. Baumberg, and C. Tejedor, Phys. Rev. B **66**, 085304 (2002).
[19] F. Tassone and Y. Yamamoto, Phys. Rev. B **59**, 10830 (1999).
[20] A. Amo, J. Lefrre, S. Pigeon, C. Adrados, C. Ciuti, I. Carusotto, R. Houdr, E. Giacobino, and A. Bramati, Nat. Phys. **5**, 805 (2009).
[21] A. Amo, S. Pigeon, D. Sanvitto, V. G. Sala, R. Hivet, I. Carusotto, F. Pisanello, G. Lemenager, R. Houdre, E Giacobino, C. Ciuti, and A. Bramati, Science **332**, 1167 (2011).
[22] K. G. Lagoudakis, M. Wouters, M. Richard, A. Baas, I. Carusotto, R. Andre, L. S. Dang, and B. Deveaud-Pledran, Nat. Phys. **4**, 706 (2008).
[23] K. G. Lagoudakis, T. Ostatnicky, A. V. Kavokin, Y. G. Rubo, R. Andre, and B. Deveaud-Pledran, Science **326**, 974 (2009).
[24] L. Ferrier, E. Wertz, R. Johne, D. D. Solnyshkov, P. Senellart, I. Sagnes, A. Lemaitre, G. Malpuech, and J. Bloch, Phys. Rev. Lett. **106**, 126401 (2011).
[25] D. Ballarini, M. de Giorgi, E. Cancellieri, R. Houdre, E. Giacobino, R. Cingolani, A. Bramati, G. Gigli, and D. Sanvitto, Nat. Commun. **4**, 1778 (2013).
[26] T. Gao, P. S. Eldridge, T. C. H. Liew, S. I. Tsintzos, G. Stavrinidis, G. Deligeorgis, Z. Hatzopoulos, and P. G. Savvidis, Phys. Rev. B **85**, 235102 (2012).
[27] A. Amo, T. C. H. Liew, C. Adrados, R. Houdré, E. Giacobino, A. V. Kavokin, and A. Bramati, Nat. Photon. **4**, 361 (2010).
[28] F. Marsault, H. Nguyen, D. Tanese, A. Lemaître, E. Galopin, I. Sagnes, A. Amo, and J. Bloch, Appl. Phys. Lett. **107**, 201115 (2015).
[29] H. S. Nguyen, D. Vishnevsky, C. Sturm, D. Tanese, D. Solnyshkov, E. Galopin, A. Lemaitre, I. Sagnes, A. Amo, G. Malpuech, and J. Bloch, Phys. Rev. Lett. **110**, 236601 (2013).
[30] D. Miller, S. Smith, and A. Johnston, Appl. Phys. Lett. **35**, 658 (1979).
[31] M. J. Adams, Solid State Electron. **30**, 43 (1987).
[32] V. Almeida and M. Lipson, Opt. Lett. **29**, 2387 (2004).
[33] H. M. Gibbs, *Optical Bistability: Controlling Light with Light* (Academic, New York, 1985).
[34] T. Tanabe, M. Notomi, S. Mitsugi, A. Shinya, and E. Kuramochi, Opt. Lett. **30**, 2575 (2005).
[35] A. Dreismann, H. Ohadi, Y. del Valle-Inclan Redondo, R. Balili, Y. G. Rubo, S. I. Tsintzos, G. Deligeorgis, Z. Hatzopoulos, P. G. Savvidis, and J. J. Baumberg, Nat. Mater. **15**, 1074 (2016).
[36] H. Sigurdsson, I. A. Shelykh, and T. C. H. Liew, Phys. Rev. B **92**, 195409 (2015).
[37] A. Baas, J. P. Karr, H. Eleuch, and E. Giacobino, Phys. Rev. A **69**, 023809 (2004).
[38] D. Bajoni, E. Semenova, A. Lemaitre, S. Bouchoule, E. Wertz, P. Senellart, S. Barbay, R. Kuszelewicz, and J. Bloch, Phys. Rev. Lett. **101**, 266402 (2008).
[39] D. Sarkar, S. S. Gavrilov, M. Sich, J. H. Quilter, R. A. Bradley, N. A. Gippius, K. Guda, V. D. Kulakovskii, M. S. Skolnick, and D. N. Krizhanovskii, Phys. Rev. Lett. **105**, 216402 (2010).
[40] C. Adrados, A. Amo, T. C. H. Liew, R. Hivet, R. Houdre, E. Giacobino, A. V. Kavokin, and A. Bramati, Phys. Rev. Lett. **105**, 216403 (2010).
[41] S. S. Gavrilov, A. V. Sekretenko, N. A. Gippius, C. Schneider, S. Höfling, M. Kamp, A. Forchel, and V. D. Kulakovskii, Phys. Rev. B **87**, 201303 (2013).
[42] N. A. Gippius, I. A. Shelykh, D. D. Solnyshkov, S. S. Gavrilov, Y. G. Rubo, A. V. Kavokin, S. G. Tikhodeev, and G. Malpuech, Phys. Rev. Lett. **98**, 236401 (2007).
[43] T. K. Paraiso, M. Wouters, Y. Leger, F. Morier-Genoud, and F. Deveaud-Pledran, Nat. Mater. **9**, 655 (2010).
[44] M. Amthor, T. C. H. Liew, C. Metzger, S. Brodbeck, L. Worschech, M. Kamp, I. A. Shelykh, A. V. Kavokin, C. Schneider, and S. Höfling, Phys. Rev. B **91**, 081404 (2015).
[45] D. Bajoni, M. Perrin, P. Senellart, A. Lematre, B. Sermage, and J. Bloch, Phys. Rev. B **73**, 205344 (2006).
[46] H. Abbaspour, S. Trebaol, F. Morier-Genoud, M. T. Portella-Oberli, and B. Deveaud, Phys. Rev. Lett. **113**, 057401 (2014).
[47] H. Abbaspour, S. Trebaol, F. Morier-Genoud, M. T. Portella-Oberli, and B. Deveaud, Phys. Rev. B **91**, 155307 (2015).
[48] H. Abbaspour, G. Sallen, S. Trebaol, F. Morier-Genoud, M. T. Portella-Oberli, and B. Deveaud, Phys. Rev. B **92**, 165303 (2015).
[49] B. Pietka, D. Zygmunt, M. Krol, M. R. Molas, A. A. L. Nicolet, F. Morier-Genoud, J. Szczytko, J. Lusakowski, P. Zieba, I. Tralle, P. Stepnicki, M. Matuszewski, M. Potemski, and B. Deveaud, Phys. Rev. B **91**, 075309 (2015).
[50] C. W. Lai, N. Y. Kim, S. Utsunomiya, G. Roumpos, H. Deng, M. D. Fraser, T. Byrnes, P. Recher, N. Kumada, T. Fujisawa, and Y. Yamamoto, Nature (London) **450**, 529 (2007).
[51] C. Ciuti, V. Savona, C. Piermarocchi, A. Quattropani, and P. Schwendimann, Phys. Rev. B **58**, 7926 (1998).
[52] See Supplemental Material at http://link.aps.org/supplemental/10.1103/PhysRevB.96.041301 for further details on the theory.